

# Droplet CFD

In an Emergent Variable Phase Turbine [1-2] (VPT) the fluid at the inlet is liquid, flashes inside the nozzle upstream of the turbine rotor, and is two-phase inside the rotor blade passage. A previous article [3] discussed calculating the trajectories of droplets inside the turbine rotor.

In the converging section of the nozzle, the pressure decreases. When it declines to the saturation pressure, vapor bubbles form. At this pressure, the liquid is the continuous phase, the vapor the dispersed phase. Above this pressure,

the calculations to develop a reduced order model that can be incorporated into traditional CFD codes and 1-D nozzle codes. Experimental work has been found for model problems to begin investigating computationally. By finding problems to study that have been investigated experimentally, the methodology used in the CFD simulations can be validated.

A starting point is to examine the flow field around a single liquid

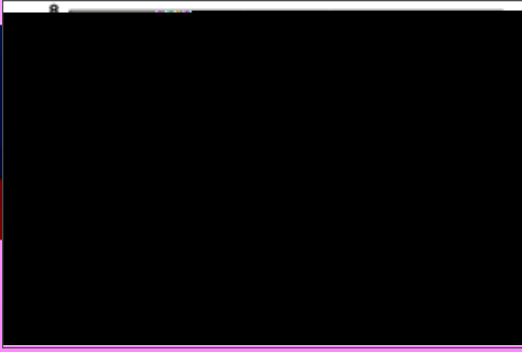


Figure 4 Drag coefficient non-dimensionalized using the deforming column frontal diameter, for a threshold value of 0.95 of the liquid volume fraction, for several different incident Mach numbers.

By using the actual column diameter instead of the initial diameter the drag coefficient shows significantly less variation during the breakup period that is simulated, Figure 4.

In the application of interest, the droplet is not in isolation, but is part of a cloud. At Sandia National Laboratory [5], experiments have been conducted on a planar shock wave impacting a curtain of solid particles.

The simulation focuses on the early stage of the experiment when the particles have not yet moved and can be assumed to be fixed in space. The 3-D particle cloud is modeled by an array of staggered cylinders, Figure 5. With the stagger arrangement used the open cross sectional area varies by less than 1.5%, Figure 6.

The volume fraction is nearly constant through the curtain. In this 2-D model, the Euler equations are solved. The numerical method implicitly contains numerical viscosity.



Figure 5 Array of staggered cylinders.

Figure 6 Open cross sectional area of the cylinder array.

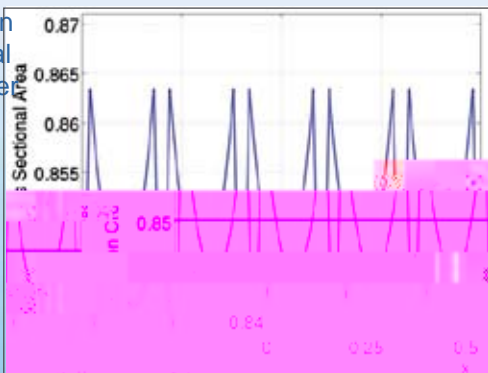


Figure 7 shows the reflected and transmitted shock waves, as well as the unsteady flow conditions both inside and behind the cylinder cloud.

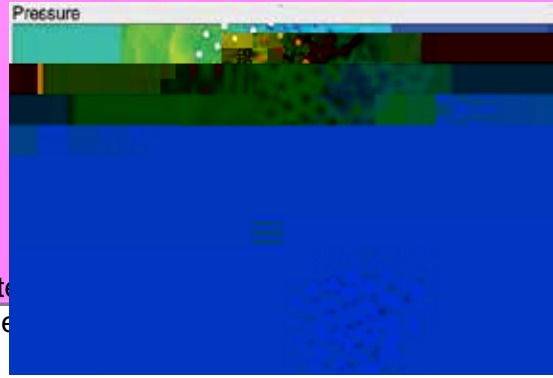


Figure 7 Flow variables of the 2-D calculation at t=3.5.

A one-dimensional model is derived from the volume-averaged Navier-Stokes equations, where the viscous stresses within the continuous phase are assumed to be negligible, but the momentum coupling terms are still considered. The 1-D model equations that were solved do not include the unclosed fluctuation terms created during the volume-averaging procedure, such as the Reynolds stress. This is a reasonable assumption in dilute multiphase flows, however, in dense flows this assumption may not be appropriate.

The miscellaneous particle forces are assumed to be included in the drag coefficient for the quasi-steady drag force on a single particle.

$$F_i^{qs} = \frac{1}{2} C_D A_p |u_i - v_i| (u_i - v_i)$$

where  $A_p$  is the particle cross-sectional area,  $C_D$  is the drag coefficient, and  $u_i$  and  $v_i$  are the continuous and dispersed phase velocities respectively. For the time period considered the particle is fixed in space, so  $v_i = 0$ . For the 2-D particle, the cross-section area is its diameter  $D_p$ . The drag coefficient  $C_D$  was determined by finding the value that best matches the reflected and transmitted shock locations and magnitudes of the 2-D solution.

Figure 8 - Figure 10 compare the solution of the 1-D model with a planar average of the 2-D result at the non-dimensionalized time of 3.5. The particle curtain is located between  $-0.5 < x < 0.5$ . For the plots of density and velocity, the 2-D results appear to oscillate around the 1-D model results for a significant portion of the solution. For these profiles, two additional cases are shown where the drag coefficient is increased and decreased by 30%. Small, yet noticeable, differences can be observed in the shock locations. This suggests that the methodology used is adequate to evaluate an overall mean drag coefficient.

continued on page 8

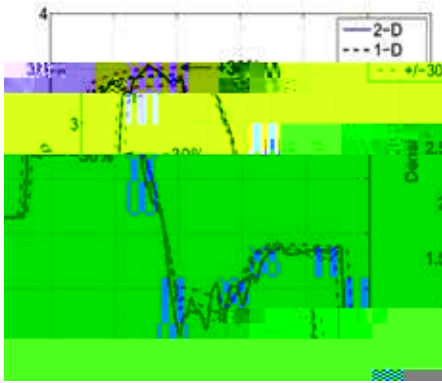


Figure 8 Comparison of the density from the 1-D model and with the planar average of the 2-D model at  $t=3.5$ . In addition for the 1-D model, the drag coefficient was varied by  $\pm 30\%$ .

Figure 9 Comparison of the velocity from the 1-D model with the planar average of the 2-D model at  $t=3.5$ . In addition for the 1-D model, the drag coefficient was varied by  $\pm 30\%$ .

In Figure 10 the planar averaged pressure in the 2-D result is consistently lower than that predicted by the 1-D model inside the particle cloud and downstream of the trailing edge until  $x 1.5$ . This is attributed to the fluctuations associated with the vortical structures (see Figure 7), which is a behavior that the 1-D model,

## CRYOGENIC INDUSTRIES TO RELOCATE HEADQUARTERS

This Fall Cryogenic Industries will relocate its headquarters offices from Murrieta, CA to Temecula, CA. The new facilities will house administrative, finance, treasury, legal, internal audit, regulatory compliance, human resources and tax functions. An announcement with the new address and telephone numbers will be made at the time of the relocation.

